Subjectivity in Calving Front Delineation in Tidewater Glacier of Antarctica

Name: Christopher Chan (s382722)

Date: 2022-07-06

Abstract

The calving front is a major control mechanism for tidewater glaciers. This is especially true for the mass balance of the Antartica Ice Sheet where it experiences a desert like climate with little percipitation change due to the sheer size of the continent. The study focus on the tidewater glaciers West Antarctic Ice Sheet and Antarctic Peninsula where they are of interest due to their past decadal retreat and response to anthropogenic climate change. The study showcases the centerline method for tracking the subjectivity of calving front delineation in the four small terminus of the Antarctic Peninsula and three larger terminus in Marie Byrd Land

Introduction

The continent of Antarctica is the largest ice mass and storage of fresh water on our planet. , Characterised by a desert climate with little percipitation, mass balance change is therefore largely determined by the rate of loss at the terminus of many tidewater glaciers around its coast. Yet, the very complex interplay between landscape, oceanic, climatic, and anthropogenic forcings (Slater et al., 2015, Slater et al., 2017, Scambos et al., 2017, Shepherd et al., 2018, Pritchard et al., 2012) have only started to be understood by glaciologist despite decades of studies. The region can be geographically divided into the Antarctic Peninsula (herein AP), West Antarctic Ice Sheet (herein WAIS), and East Antarctic Ice Sheet (herein EAIS) (Gardner et al, 2018).

Study Area

There are 7 Areas of Interest for this study. Congregating in the WAIS and AP, this region of the Antarctica have been the focus of calving front studies for the last two decades (Gardner et al., 2017). This is due to the rapid retreat and intricate dynamics with the Circumpolar Deep Water and complicated bythmetric topography, which the WAIS contributed 88% of increased discharge from the continent (Baumhoer et al., 2018, Scambos et al., 2017, Prichart et al., 2017, Shepherd et al., 2018) (*see figure 1 & 2*).

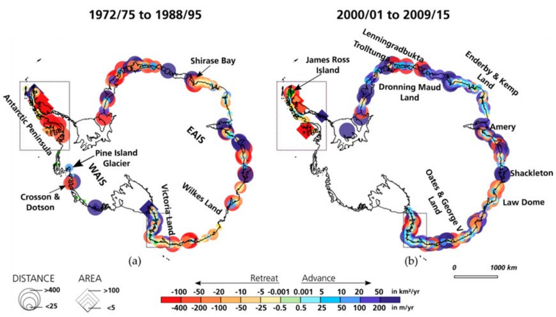

Figure 1: Advance and retreat of tidewater glaciers around Antarctica (Baumhoer et al., 2018).

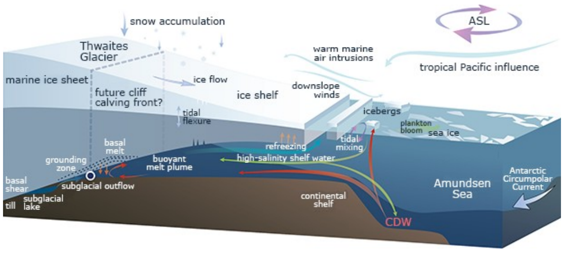

Figure 2: Schematic diagram of interaction between tidewater glacier and Circumpolar Deep Water (Scambos et al., 2017).

Of the seven tidewater glaciers investigated, four were located in the AP provided from Sentinel-2 optical images (*see Figure 3.*) , while the other three were Sentinel-1 SAR backscatter in the Amundsen Sea area, Marie Byrd Land (herein MBL) (*see Figure 4.*).

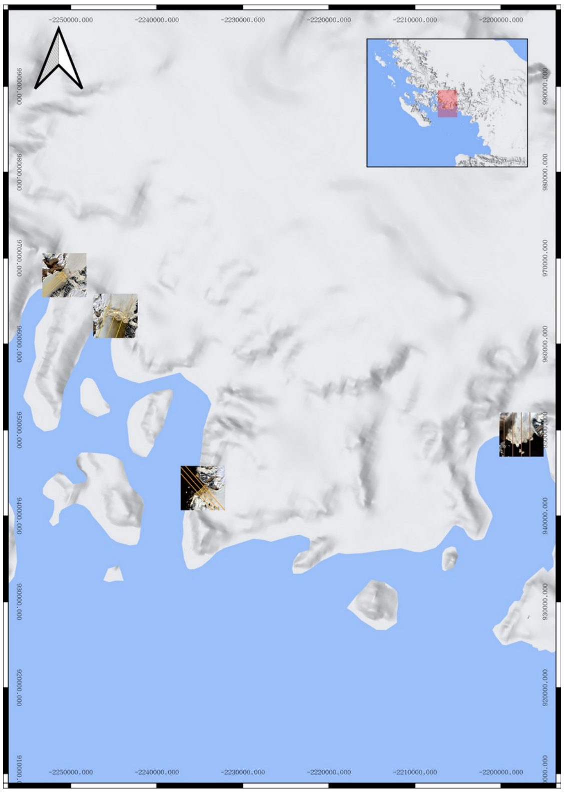

Figure 3: Overview map of interested glaciers in Antarctic Peninsula.

Figure 4: Overview map of interested glaciers in Marie Byrd Land.

The AP is one of the warmest region in Antarctica, and naturally most responsive to anthropogenic climate change, with a 25-year average mass balance of -20 ± 15 Gt yr^{-1} at 2018 (Gardner et al., 2018, Vaughan et al. 2003).

The other Area of Interest Amundsen Sea area of MBL is a vast collections of calving fronts but have been experiencing rapid retreat. In particular within this study area Land and Thwaites Glaciers are known as ice stream, where collapse of the calving front causes a considerable increase in flow velocity (Cuffrey & Paterson, 2010)

State-of-the-art literature review

Given the importance of calving front that controls the mas balance of the Antarctic Ice Sheet, tracking the advance and retreat of the calving front around the coastline of Antarctica, Prior to the data-drive paradigm shift of feature extraction, which applies extensively to any Computer Vision and remote sensing task, calving front and centerline delineation were often performed manually. In Lea et al. (2014) review of calving front measurements methods, it was suggested the centerline could be derived in 3 ways: 1. Manual estimation, 2. Topographic centerline, 3. Fastest flow axis. As the centerline method is one of the simplest, it is quick to implement. However, it does not account for the full complexity of a dynamic terminus, especially with the width-average terminus change and prone to suggesting an over- and underestimation. It is perhaps more suitable for land-terminating glaciers than tidewater glaciers.

Novel methods of deriving centerlines (e.g. Kienholz et al., 2014, Zhang et al., 2021) might provide more tailorded approach to creating centerlines that circumvent these issues, but it will be beyond the scope of this study to discuss such works.

Regarding recent advances in calving front delineation, data-driven approach have been dominating the literatures (e.g. Zhang et al., 2019, Baumhoer et al., 2019, Cheng et al., 2021)

Methods

Calving fronts for each glacier were manually delineated by our fellow classmates for this coursework, initially resulting in four calving fronts delineation per glacier. However due to the variance in familiarity with glaciology, some of the delineation were unusable.

Standardised spaced apart centerlines are first drawn parallel to the direction of flow, or perpendicular to the calving front terminus. From which the difference in calving front, whether the study is timeseries or subjectivity in delineation are measured against. Therefore, the higher density of centerlines provides greater spatial resolution (Baumhoer et al., 2018, Lea et al., 2014). This study aim to showcase the centerline methodology and the resulting differences between calving front delineations of smaller-scale Optical based images and larger-scale SAR based images.

Perpendicular centerlines were first created in QGIS to the specifications of (*see Table 1. & Figure 5.*) for each imagery. Due to the drastically different size of the glaciers, the spacing between centerlines are different between the glaciers.

Table 1: Specification of centerlines parallel to the terminus of interested tidewater glaciers

Glacier	Fronts delineated	Centerline count	Spacing	Mean std.	Imagery
Forbes	n = 4	3	1 km	16.292	Optical
Marvodol	n = 4	4	0.25 km	26.757	
McMorrin	n = 4	3	0.5 km	200.99	
Neny	n = 4	4	1 km	429.427	
Getz	n = 3	17	5 km	63.849	SAR
Thwaites	n = 4	15	5 km	2003.189	
Land	n = 2	7	5 km	NaN	

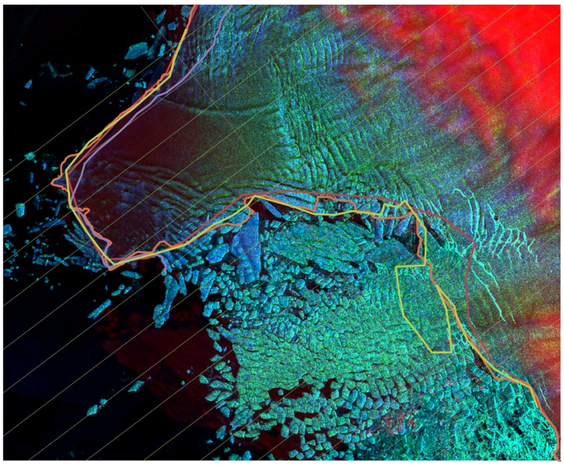

Figure 5: SAR backscatter of Thwaites Glacier, MBL with 5 km spaced centerline and delineated calving fronts.

A python script provided by Baumhoer C. (2021) calculates the deviation of the calving fronts against the first input for each centerline. Basic statistics were calculated from the results generated. This means that the algorithm require the number of fronts delineated to be n > 2.

Results

In general, no concrete conclusion could be suggested as to whether our classmates had an easier in delineating Optical based or SAR based glaciers in the mean standard deviations of the combined calving fronts (*see Table 1.*). However, there is a general trend where confusion do often occur. Standard deviation in calving fronts delineations is not consistent through the centerlines, they are often times subjected to drastic difference (*see Figure 6 & 7*).

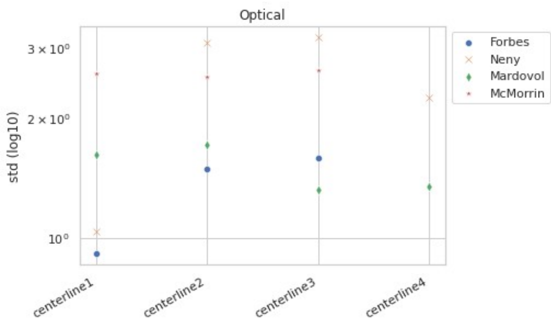

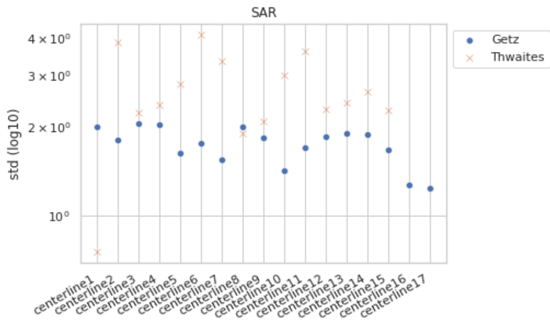

Figure 6 & 7: Standard deviation of calving fronts for each centerline in AP (Optical) and MBL (SAR).

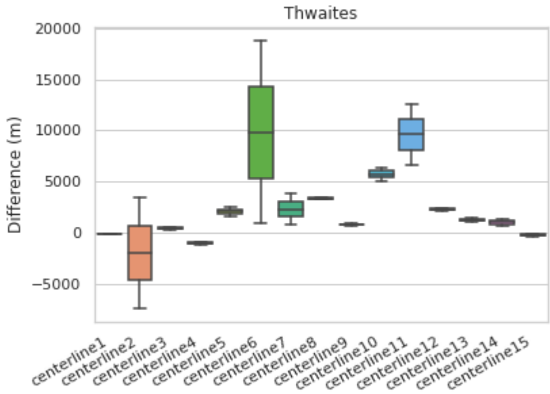

Figure 8: Box and whisker plot for difference in each centerline of Thwaites Glacier, MBL.

Discussion

Take the box and whisker plot of Thwaites glacier as an example (*see Figure. 5 & 8*), theres a drastic increase in difference range when our fellow classmates encounter ambiguous calving front such as in *centerline 12*, where it is not obvious whether the ice melange ends and non-ice melange or collection of calved icebergs begins. Meanwhile in *centerline2 and centerline6*, the large difference in the boxplot actually showcase the disadvantage of the centerline methodlogy , while delineation were quite close together, perpendicular mono-directional centerline register sharp difference in distance because the calculation does not consider width-average terminus change as mentioned before.

The case of *centerline 2 and 6* where the difference increase where the algorithm neglected width-average terminus change is much more prominent in SAR based glacier. This is probably due to the much larger scale and thereby coplexity of the interested calving fronts in MBL as oppose to the much smaller and geomorphologically constrainted calving fronts of AP.

Conclusion

In conclusion, this simple study reviewed and showcased the advantages and disadantages of the centerline method for measuring calving fronts delineation. A brief literature review was conducted regarding the impotance of calving front as a control for tidewater glaciers, as well as the state of the art for centerline derivation and calving front extraction. The result of this study concluded that in order to successfully carry out calving front delineation using the centerline methods, one need to both account for the knowledge of the digitiser and compensate for the pros and cons of the centerline method. It is therefore recommended that in future studies, different methodlogy shall be employed given the geometry of not only the calving front, but also the general shape of the glacial terminus.

Bibliography

Baumhoer, Celia A, Andreas J Dietz, Stefan Dech, and Claudia Kuenzer. 2018. 'Remote Sensing of Antarctic Glacier and Ice-Shelf Front Dynamics—A Review'. *Remote Sensing* 10 (9): 1445.

Baumhoer, Celia A., Andreas J. Dietz, Christof Kneisel, and Claudia Kuenzer. 2019. 'Automated Extraction of Antarctic Glacier and Ice Shelf Fronts from Sentinel-1 Imagery Using Deep Learning'. *Remote Sensing* 11 (21): 2529.

Baumhoer, Celia A., Andreas J. Dietz, Christof Kneisel, Heiko Paeth, and Claudia Kuenzer. 2021. 'Environmental Drivers of Circum-Antarctic Glacier and Ice Shelf Front Retreat over the Last Two Decades'. *The Cryosphere* 15 (5): 2357–81. https://doi.org/10.5194/tc-15-2357-2021.

Cheng, Daniel, Wayne Hayes, Eric Larour, Yara Mohajerani, Michael Wood, Isabella Velicogna, and Eric Rignot. 2021. 'Calving Front Machine (CALFIN): Glacial Termini Dataset and Automated Deep Learning Extraction Method for Greenland, 1972–2019'. *The Cryosphere* 15 (3): 1663–75.

Cuffey, Kurt M, and William Stanley Bryce Paterson. 2010. *The Physics of Glaciers*. Academic Press.

Depoorter, M. A., J. L. Bamber, J. A. Griggs, J. T. M. Lenaerts, S. R. M. Ligtenberg, M. R. van den Broeke, and G. Moholdt. 2013. 'Calving Fluxes and Basal Melt Rates of Antarctic Ice Shelves'. *Nature* 502 (7469): 89–92. https://doi.org/10.1038/nature12567.

Garbe, Julius, Torsten Albrecht, Anders Levermann, Jonathan F. Donges, and Ricarda Winkelmann. 2020. 'The Hysteresis of the Antarctic Ice Sheet'. *Nature* 585 (7826): 538–44. https://doi.org/10.1038/s41586-020-2727-5.

Gardner, Alex S., Geir Moholdt, Ted Scambos, Mark Fahnstock, Stefan Ligtenberg, Michiel van den Broeke, and Johan Nilsson. 2018. 'Increased West Antarctic and Unchanged East Antarctic Ice Discharge over the Last 7 Years'. *The Cryosphere* 12 (2): 521–47. https://doi.org/10.5194/tc-12-521-2018.

Holland, David M., Robert H. Thomas, Brad de Young, Mads H. Ribergaard, and Bjarne Lyberth. 2008. 'Acceleration of Jakobshavn Isbræ Triggered by Warm Subsurface Ocean Waters'. *Nature Geoscience* 1 (10): 659–64. https://doi.org/10.1038/ngeo316.

Joughin, I., B. E. Smith, D. E. Shean, and D. Floricioiu. 2014. 'Brief Communication: Further Summer Speedup of Jakobshavn Isbræ'. *The Cryosphere* 8 (1): 209–14. https://doi.org/10.5194/tc-8-209-2014.

Khazendar, Ala, Ian G. Fenty, Dustin Carroll, Alex Gardner, Craig M. Lee, Ichiro Fukumori, Ou Wang, et al. 2019. 'Interruption of Two Decades of Jakobshavn Isbrae Acceleration and Thinning as Regional Ocean Cools'. *Nature Geoscience* 12 (4): 277–83. https://doi.org/10.1038/s41561-019-0329-3.

Kienholz, C., J. L. Rich, A. A. Arendt, and R. Hock. 2014. 'A New Method for Deriving Glacier Centerlines Applied to Glaciers in Alaska and Northwest Canada'. *The Cryosphere* 8 (2): 503–19. https://doi.org/10.5194/tc-8-503-2014.

Lea, James M., Douglas W. F. Mair, and Brice R. Rea. 2014. 'Evaluation of Existing and New Methods of Tracking Glacier Terminus Change'. *Journal of Glaciology* 60 (220): 323–32. https://doi.org/10.3189/2014JoG13J061.

Pritchard, HDx, Stefan RM Ligtenberg, Helen A. Fricker, David G. Vaughan, Michiel R. van den Broeke, and Laurence Padman. 2012. 'Antarctic Ice-Sheet Loss Driven by Basal Melting of Ice Shelves'. *Nature* 484 (7395): 502–5.

Scambos, T. A., R. E. Bell, R. B. Alley, S. Anandakrishnan, D. H. Bromwich, K. Brunt, K. Christianson, et al. 2017. 'How Much, How Fast?: A Science Review and Outlook for Research on the Instability of Antarctica's Thwaites Glacier in the 21st Century'. *Global and Planetary Change* 153 (June): 16–34. https://doi.org/10.1016/j.gloplacha.2017.04.008.

Shepherd, Andrew, Erik Ivins, Eric Rignot, Ben Smith, Michiel van den Broeke, Isabella Velicogna, Pippa Whitehouse, et al. 2018. 'Mass Balance of the Antarctic Ice Sheet from 1992 to 2017'. *Nature* 558 (7709): 219–22. https://doi.org/10.1038/s41586-018-0179-y.

Slater, Donald Alexander, Peter W Nienow, Daniel N Goldberg, Tom Ralph Cowton, and Andrew John Sole. 2015. 'Co-Evolution of Tidewater Glacier Calving Front Morphology and Submarine Melt Rates in a High Resolution Ocean Model'. In , 2015:C13E-02.

Slater, Donald Alexander, PW Nienow, DN Goldberg, TR Cowton, and AJ Sole. 2017. 'A Model for Tidewater Glacier Undercutting by Submarine Melting'. *Geophysical Research Letters* 44 (5): 2360–68.

Vaughan, David G., Gareth J. Marshall, William M. Connolley, Claire Parkinson, Robert Mulvaney, Dominic A. Hodgson, John C. King, Carol J. Pudsey, and John Turner. 2003. 'Recent Rapid Regional Climate Warming on the Antarctic Peninsula'. *Climatic Change* 60 (3): 243–74.

Zhang, Dahong, Xiaojun Yao, Hongyu Duan, Shiyin Liu, Wanqin Guo, Meiping Sun, and Dazhi Li. 2021. 'A New Automatic Approach for Extracting Glacier Centerlines Based on Euclidean Allocation'. *The Cryosphere* 15 (4): 1955–73. https://doi.org/10.5194/tc-15-1955-2021.

Zhang, Enze, Lin Liu, and Lingcao Huang. 2019. 'Automatically Delineating the Calving Front of Jakobshavn Isbræ from Multitemporal TerraSAR-X Images: A Deep Learning Approach'. *The Cryosphere* 13 (6): 1729–41.